Journal of Engineering and Applied Sciences 11 (Special Issue 2): 3193-3202, 2016
ISSN: 1816-949X


# Investigating the Effect of Composite Stirrups in T-shaped Concrete Connections

Iman Bahrami Chegeni and Ahmad Dalvand
Faculty of Engineering, Lorestan University, Khorramabad, Iran

**Abstract:** The usage of composite materials has been increasing over the recent years. Characteristics such as high tensile resistance, erosion resistance and cost effectiveness are the reason of such trend. Using composite materials in concretes exposed to corrosive environments helps to increase the durability of the structure. The stirrups of a concrete structure, compared to longitudinal bars, due to closeness to concrete surface and less diameter are expected to have more defects in corrosive and acidic environments. In this study, an experimental and a finite element investigation is carried out on hysteresis behavior of T concrete connections for the effect of composite stirrup's distance in the experimental part, a concrete connection is tested to calibrate the finite element model. Following that the experimental model was compared to and verified by the finite element model, using the finite element software ANSYS. Two groups of concrete connections, each including two connections are modeled by ANSYS. In each group, the variable is the steps of composite stirrups. Based on the results, connections with dense stirrup has 12% more capacity in compare to non-dense tied connections.

**Key words:** Composite stirrup, finite element, energy absorption, T connections, erosion resistance

## INTRODUCTION

Using composite stirrups instead of steel stirrups is increasing because of their high resistance against corrosive substances. The usage of bars made from CFRP and GFRP fibers for longitudinal and transvers bars and FRP sheets to apply in bridges and dowels and buildings is increasing (Fukuyama *et al*., 1995; Sharbatdar and Kazem, 2003; Theodorakopoulos and Swamy, 2008). Besides the usage of FRP fibers to strengthen concrete beams and rehabilitating concrete connections has increased for during the recent decades (Ceroni, 2010; Si-Larbi *et al*., 2012; ACI Committee 318, Canadian Standards Association, 2002; Mahini and Ronagh, 2010; Ghobarah and Said, 2002; Mukherjee and Joshi, 2005). And several design codes are issued to use FRP fibers in concrete structures. ACI Committee 440.2R-02; Nanni, 2001) because of high prices and low ductility, using longitudinal FRP bars is not cost-effective in small projects. On the other hand having bigger diameters besides having a thicker cover of concrete, longitudinal bars in compare to transvers bars are less prone to corrosion. Due to the aforementioned reasons longitudinal bars are not affected by corrosion as much as transvers bars, stirrups have a major effect on hysteresis behavior of the structure and its energy absorption and dissipation. Corrosion and damages induced to stirrups because of their adjacency to sulfate and chloride environments leads to not only reduction in structure's capacity but its resistance to seisminic loads. Concrete buildings that are constructed without considering seismic, generally known as frames designed for gravitational loads are very vulnerable to horizontal loads of earthquake. A major portion of these damages which can lead to collapse and failure of the structure are due to large spacing of stirrups and omitting the ductility requirements of the building. In the United States such earthquake regulation codes for concrete frames were released on 1971 in code ACI-318 (ACI Committee 318, 2002). The requirements on ductility of concrete structures is mostly about the usage of steel stirrups. There is limited studies on the effect of FRP stirrup's spacing on the earthquake behavior of the concrete structure. ACI codes in ACI-4400-1R do not address ductility on structures with FRP stirrups (ACI Committee 440.2R-02, 2002). Most studies are about the web stirrup's role on the behavior of concrete connections with longitudinal FRP bars (Sharbatdar *et al*., 2011).

**Characteristics of experimental specimen:** The studied specimen is modeled on 1:2 scale. The height and width of column is 250 and 200 mm and those of the beam are 200 and 250 mm, respectively which is around half of the real model. The experimental models have steel longitudinal bars and CFRP stirrups. This connection is used as the validation reference of the FEM Model.

As shown in Fig. 1, the column has for reinforcement and the beam has for both top and bottom of the

**Corresponding Author:** Iman Bahrami Chegeni, Faculty of Engineering, Lorestan University, Khorramabad, Iran

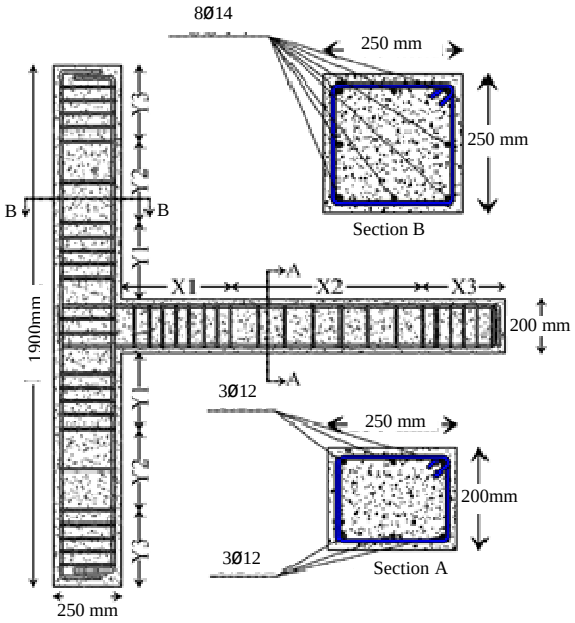


| Specimen zone | Ref. |
|---|---|
| X1 450 mm | FRP stirrup at 50 mm |
| X2 650 mm | FRP stirrup at 100 mm |
| X3 300 mm | FRP stirrup at 50 mm |
| Y1 275 mm | FRP stirrup at 50 mm |
| Y2 300 mm | FRP stirrup at 150 mm |
| Y3 275 mm | FRP stirrup at 50 mm |

Fig. 1: Connection details

Table 1: Experimental specimen carachteristics

| Specimen | Column's rebar count | Beam's rebar count | | Critical zone's stirrups spacing | | Non-critical stirrups zone | | The number of stirrup's at connection | Stirrup's material |
|---|---|---|---|---|---|---|---|---|---|
| | | Top | Bottom | Beam | Column | Beam | Column | | |
| Ref | 8 | 3 | 3 | 50 | 50 | 100 | 150 | 2 | CFRP |

study. The stirrups of the reference specimen at the critical zone (ductility conditions) have 450 mm length and spaced at 50 mm steps, this changes to 100 mm at areas out of this zone. The connection details are shown in Table 1. Portland cement type 2 was used for concrete. f'c of the concrete is 30 MPa. The maximum aggregate dimension is 10 mm and slump was held at 80 mm. Ribbed bars are used for reinforcing all three specimen. The characteristics of the steel rebar are listed in Table 2. Stirrups used in this study are CFRP their characteristics such as shown in Table 3.

**FRP stirrups design:** Designing the cross section of FRP stirrups is done by using the equivalent cross section of steel stirrups. To do this, it was assumed that the FRP stirrups equal to steel stirrups with 28.3 $m^2$ and yielding resistance of 260 MPa are embedded in the connections. As stated in design codes the shear capacity of steel stirrups is calculated as:

$$V_s = \frac{A_{sv} F_y d}{S_s} \quad (1)$$

In which $A_{sv}$ $F_y$, d and $S_S$ are the sum of stirrup leg's cross-section area, yielding resistance of steel rebar, effective height of cross-section and spaces between steel stirrups, respectively. In case of using FRP stirrups as mentioned in ACI-440-1R, the share of the FRP stirrups from the shear is calculated as:

Table 2: Specifications of the connection rebar

| Rebar's diameter (mm) | Used as | Yielding resistance (MPa) | Ultimate resistance (MPa) |
|---|---|---|---|
| 14 | Column longitudinal rebar | 408 | 470 |
| 12 | Beam longitudinal rebar | 354 | 542 |

Table 3: Characteristics of carbon fiber plates

| Product's name | Type of fiber | Tensile strength (MPa) | Elasticity module (GPa) | Ultimate strain (%) | Thickness of each fiber's layer (mm) |
|---|---|---|---|---|---|
| YC-N200 | High resistance carbon | 3550 | 235 | 1/5 | 0/11 |

$$V_f = \frac{A_{fv} f_{fv} d}{s} \quad (2)$$

Where:

$V_f$ = The shear load share of FRP stirrups
$A_{fv}$ = The sum of the cross section stirrup legs
s = Space between stirrups
$f_{fv}$ = the stress in FRP stirrups

As proposed in ACI-440-R1, the stress in FRP stirrups can be stated as:

$$f_{fv} = 0.004E_f \quad (3)$$

In which $E_f$ is the elasticity module of FRP stirrups. ACI-440-1R advises to have a minimum of shear stirrups in the cross-section equal to relation 4.

$$A_{fv,min} = 0.35\frac{b_w s}{f_{fv}} \quad (4)$$

In which $b_w$is beam's width. To design the equal FRP stirrups based on relations represented in the codes, the required cross-section area of FRP stirrups based on relation 5 and 0.4% strain are represented in Table 4 and 5:

$$A_f = \frac{A_s F_y}{0.004E_f} \quad (5)$$

Where:
$A_s$ = A single stirrup leg's cross-section area
$A_f$ = The equivalent cross-section are of FRP stirrups

In addition, the steel rebar that is considered to design FRP stirrups has 6 mm diameter and yielding strength of 260 MPa which equal amount of FRP stirrups were used instead.

**The experiment system set:** The experiment set is shown in Fig. 2. To apply hysteresis load on both ends of the beam two 200 kN actuators where installed horizontally at the top of the specimen and to apply axial load to the column a 500 kN actuator is located at the end of the column and the other end is restrained as pinned support. The arm of loading point to the connection side is 1250 mm and also the center to center distance of supports is 1500 mm. The applied constant axial load of 350 kN on the column through the experiment is 20% of its capacity.

Table 4: Comparing experimental and FEM Models

| | | | | | Difference percentage compared to experimental model | | | |
|---|---|---|---|---|---|---|---|---|
| Specimen | $\Delta_Y$ (mm) | $M_y$ (kN.m) | $\Delta_n$ (mm) | $M_n$ (kN.m) | $\Delta_y$ (%) | $M_y$ (%) | $\Delta_n$ (%) | $M_n$ (%) |
| Experimental | 9/89 | 12/13 | 85 | 31 | 6/7 | 5/2 | 3/6 | 10/5 |
| FEM | 10/56 | 12/76 | | 81/9 | 34/21 | | | |

Table 5: Dimensions and details of longitudinal rebar of the connections

| | | Beam dimensions (mm) | | Column dimensions (mm) | | | |
|---|---|---|---|---|---|---|---|
| Group No. | Specimen name | Height | Width | Height | Width | Beam rebar at top and bottom | Column rebar |
| 1 | J1D | 400 | 500 | 500 | 500 | 4ϕ20 | 12ϕ20 |
| | J1U | 400 | 500 | 500 | 500 | 4ϕ20 | 12ϕ20 |
| 2 | J2D | 550 | 650 | 650 | 650 | 5ϕ25 | 16ϕ25 |
| | J2U | 550 | 650 | 650 | 650 | 5ϕ25 | 16ϕ25 |

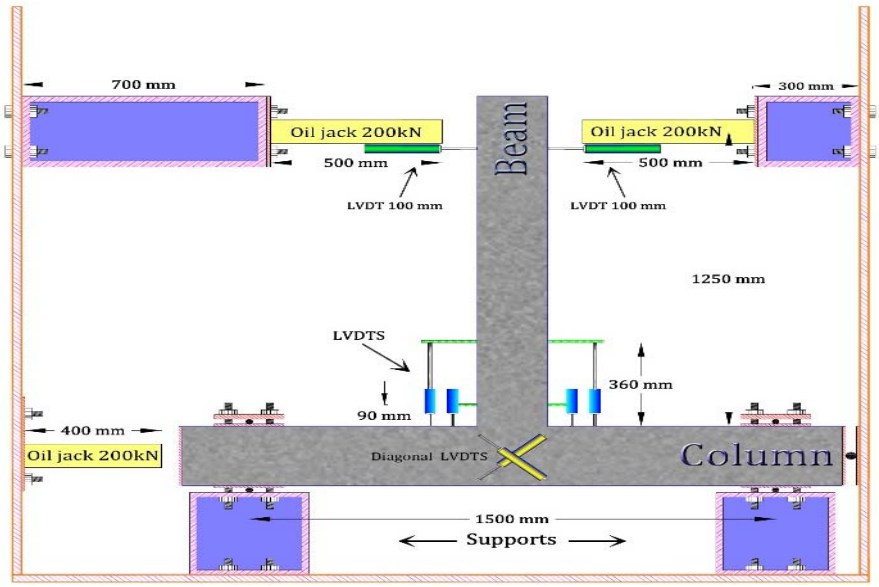


Fig. 2: Set up details of the experiment

which is calculated by the following relation. The horizontal load, applied according to displacement control method, started by 3 cycles of 0.5% until elastic flexural cracks appeared. Following that three cycles of 1% were applied. The following steps included three cycles at each increasing loading round. To record the information of concrete connection, some strain gauges were installed at stirrup leg of the panel zone and three points on longitudinal rebar of column and beam and also the two last stirrups of the beam.

**Behavior of the experimental specimen:** Figure 3, the moment-drift curve of the reference specimen is depicted. The curve is illustrating the steady behavior of connections to the 7% drift point. In the experimental specimen, plastic hinges were formed due to implying weak beam-strong column idea in designing process. Because of the stronger column than beam, less plastic strains were appeared at panel zone and less failure at the beam area. During applying all displacements, no resistance reduction is observed and the specimen passed all the above displacements with no resistance reduction. The reference specimen took an ultimate moment of 31.3 KN.m at 85 mm of ultimate displacement. As seen in the diagram the reference specimen has a ductile behavior. The first yielding of beam's longitudinal bars happened at 15.2 kN.m moment and 9.89 mm displacement for the reference specimen. The specimen ductility is defined based on ultimate displacement to yielding displacement. This is 8.9 for the experimental specimen. The initial cracking of the experimental specimen happened at 1% drift at panel zone. Figure 4 the diagonal strain of panel zone which is measured by the diagonally embedded LVDTs is depicted. Based on that Fig. 4, the maximum compression strain at the panel zone for the end of the loading is 1.8%. Furthermore, the maximum tensile strain at the end of loading is calculated to be 1.78%. The experimental specimen at the end of loading is shown in Fig. 5.

**The strain of connection stirrups:** Figure 6 the strain of the first stirrups at 50 mm distance from column side is shown against the implied moment. Based on this figure the strain of CFRP stirrups at the end of loading is equal to 0.88% for the reference specimen. Figure 7 the strain of panel zone stirrups is plotted based on implied moments to the connection. The maximum strain for reference specimen at the end of loading is 0.24%. Figure 8 the moment-strain curve of the first stirrups of the column at the 50 mm distance from beam side is plotted for experimental specimen. Based on this figure the maximum strain of the stirrups in the reference specimen at the end of loading is 0.51%.

**Moment-rotation behavior of the experimental specimen:** Moment-rotation figure depicts accurately the flexural characteristic for a reinforced concrete section. For a given concrete section with defined distribution of longitudinal reinforcement and for a certain axial load, this curve provides the moment that the beam has at each curvature compared to its initial condition. To define moment-rotation curve, the geometry of the section, rebar position and their diameter, concrete and steel's stress-strain curves, the implied axial load and the direction of the moment should be known hence, the curvature is varying at each stage and equals to the

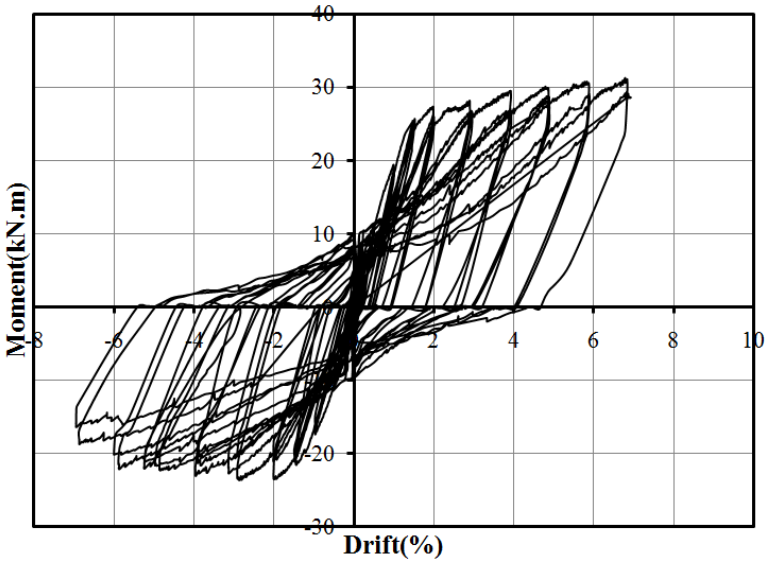


Fig. 3: Moment-displacement curve of experimental specimen

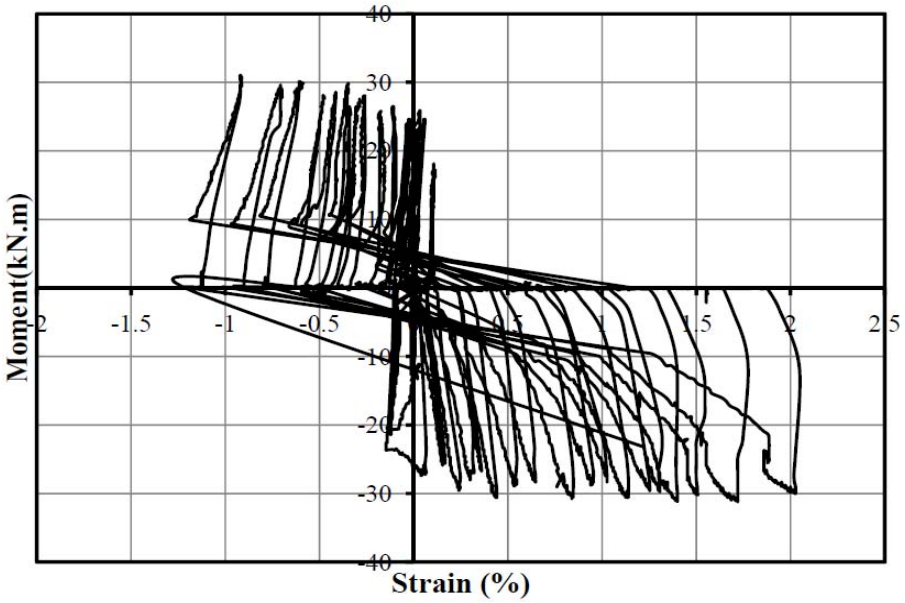


Fig. 4: Compression and tension strain of diagonal LVDTs at plate zone

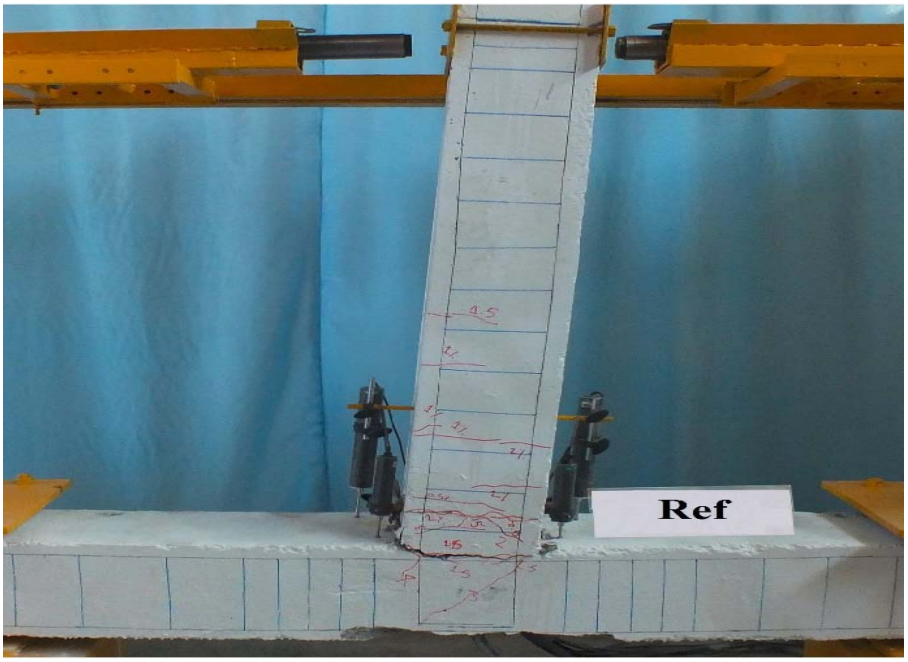


Fig. 5: Connections at the end of loading

compression strain to the neutral axi'ss height which is derivable based on experimental information recorded at each stage. Figure 9, the moment-rotation of connection beam's section at 50 mm distance from column's side is shown. The maximum curvature for the reference specimen is 0.058 radian. The connection's energy absorption curve based on imposed drift is plotted in Fig. 10. Based on this curve the reference specimen has relatively low energy absorption until 1.5% drift in such way that at this drift the energy absorption is equal to 388 kN.mm while the maximum energy absorption for this reference letter is 3610 kN.mm at 7% drift.

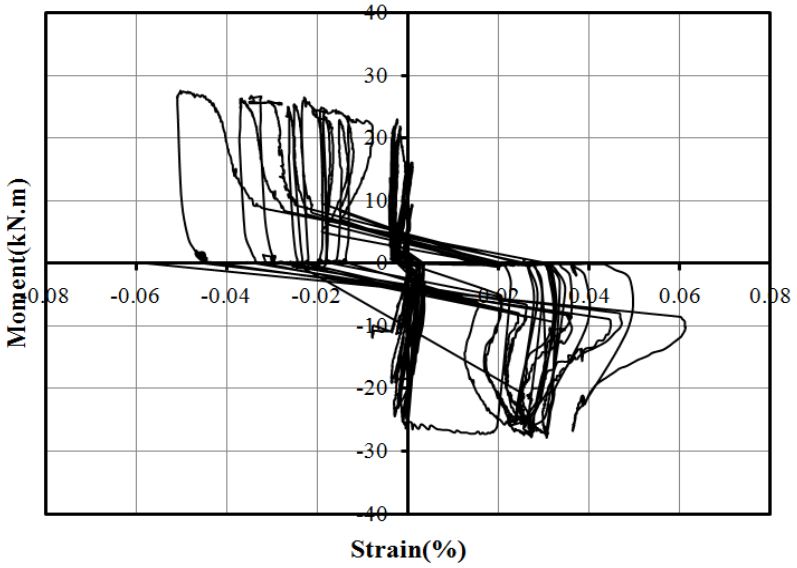


Fig. 6: Strain of the first stirrup at the connection-JFD connection

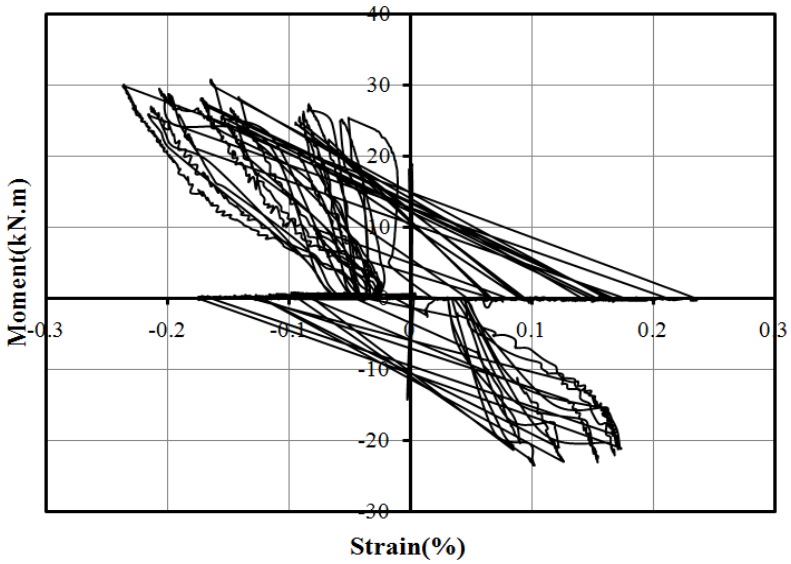


Fig. 7: Strain of stirrups at panel zone

**Stiffness and energy absorption of the experimental specimen:** Figure 11 the stiffness changes of the reference specimen is plotted against displacement of the beam's end. As it could be seen, the stiffness changes curve is descending. The stiffness is defined as the steep of the fitted curve of force-displacement curve.

**Validation of the FEM Model:** To validate the results from ANSYS Software, the FEM Model of JFD was built. To model concrete Solid 65 element was used. This element has the ability of modeling cracking and crashing at tension and compression. This 8 node element has three degrees of freedom at each node as transmission for x, y and z directions. To model the longitudinal bars and FRP stirrups the element LINK8 was chosen this element with three freedom degrees at each end has the ability to bear tension and compression but no flexural load. To model the support and loading plates element 45 was used. Strain monitoring was used to control the rupture of FRP stirrups. Using the dimensions of the experimental model, the FEM Model of the concrete beam was built and meshed for the analysis by ASYSY as shown in Fig. 12.

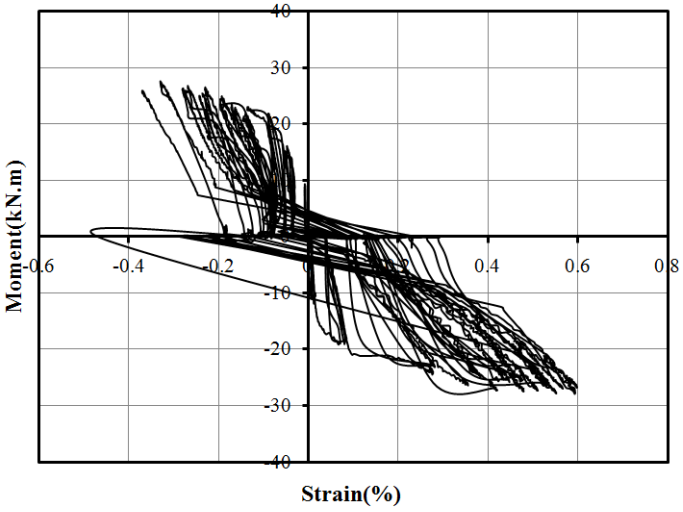


Fig. 8: Moment-strain curve of the column's first tie

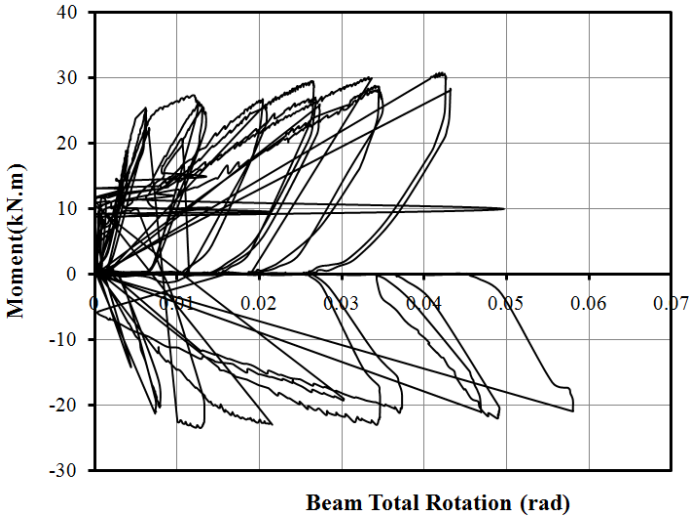


Fig. 9: Moment-rotation curve

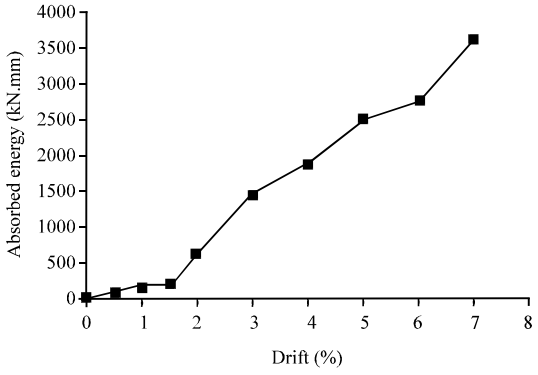


Fig. 10: Energy absorption of experimental specimen

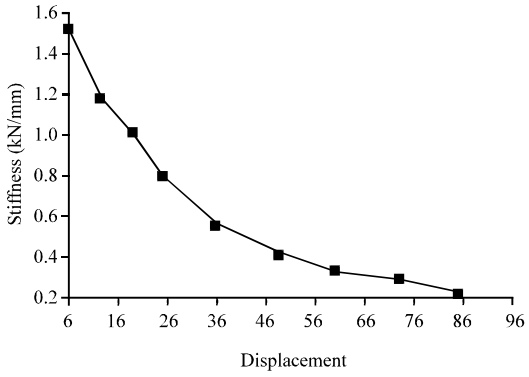


Fig. 11: Changes of stiffness of the connection based on displacemnt

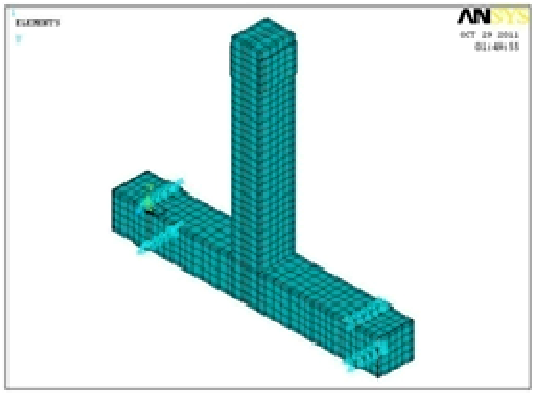

Fig. 12: FEM Model of experimental specimen JFD

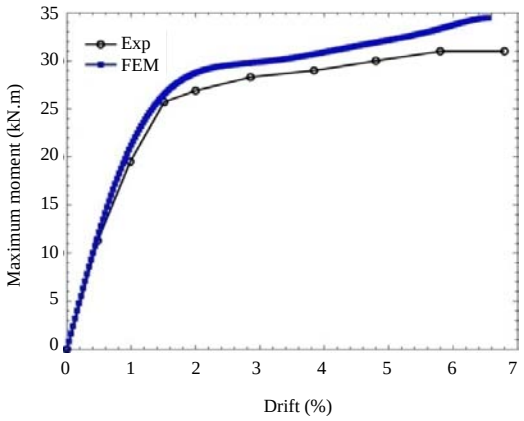


Fig. 13: Load-displacement diagram of experimental model and finite element of reference specimen

Figure 13 load-displacement curves of FEM and experimental models are shown. As shown in Fig. 13 they confirm each other well. The results of experimental and finite element models are listed in Table 4. Based on this table the experimental and finite element models has only 10% difference of which it is equal to 6.7% for the displacement that the first yielding of longitudinal rebar is detected and 5/2% for the yielding load of connection beam's longitudinal rebar, 3/6% for ultimate displacement and 10.5% for the ultimate load of the connection.

**The built finite element models:** To investigate the effect of FRP stirrups on reinforced concrete connection's behavior, 2 groups of concrete connections with different dimensions and reinforcement were modeled. Each group included two connections which have similar dimensions and longitudinal reinforcement. In each group, the first connection has FRP stirrups with ductile conditions and the second connection had FRP stirrups with non-ductile conditions. In other words the spacing between FRP stirrups of the second connection is twice of the first connection. The FEM specimen's concrete has a compression strength equal to 30 MPa and longitudinal rebar specification like the experimental specimen. The dimensions are chosen to imply weak beam-strong column idea. The dimensions and number of longitudinal rebar of modeled connections are listed in Table 5.

Also, in Table 6, the cross-section area of FRP stirrups and their spacing at ductile and non-ductile zones is shown. The length of ductile and non-ductile zones in column and beam of the first and second group is 800 and 500 mm, respectively. Furthermore, the total length beam and column at each for model is 2000 and 3500 mm, respectively and also the center to center distance of two supports is 3100 mm at Fig. 14 the connections specifications is illustrated. In Fig. 15, two of FEM Models

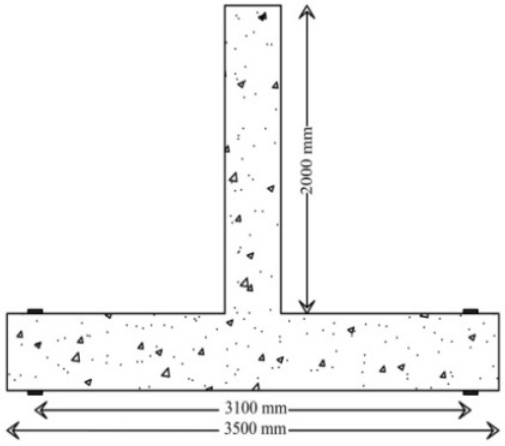


Fig. 14: The general dimensions of FEM Models

are shown. Based on this figure there are plates located at both sides and top and bottom of the column as supports.

**Load-displacement behavior of FEM Models:** The studied connections are imposed to ascending loading at the end of beam. Load-displacement of four specimen are shown in Fig. 16. The loading of all specimens is done until till 7% drift with displacement equal to 140 mm. Based on analysis for both connection groups with FRP stirrups, in each group those specimen with FRP stirrups and ductile conditions at critical zones have higher load bearing capacity than connections with FRP stirrups with non-ductile conditions. In the first group specimen J1D, has the maximum moment of 135/6 kN.m which is 8.6% more than J1U specimen. Similarly, at the second group the J2D connection has the maximum moment of

Table 6: Cross-section of FRP stirrups and their spacing

| Group No. | Specimen name | Single side of FRP stirrup's cross-section area (mm) | Stirrups spacing at ductile zone | Stirrups spacing at non-ductile zone |
|---|---|---|---|---|
| 1 | J1D | 6 | 100 | 200 |
| | J1U | 6 | 200 | 200 |
| 2 | J2D | 8 | 150 | 300 |
| | J2U | 8 | 300 | 300 |

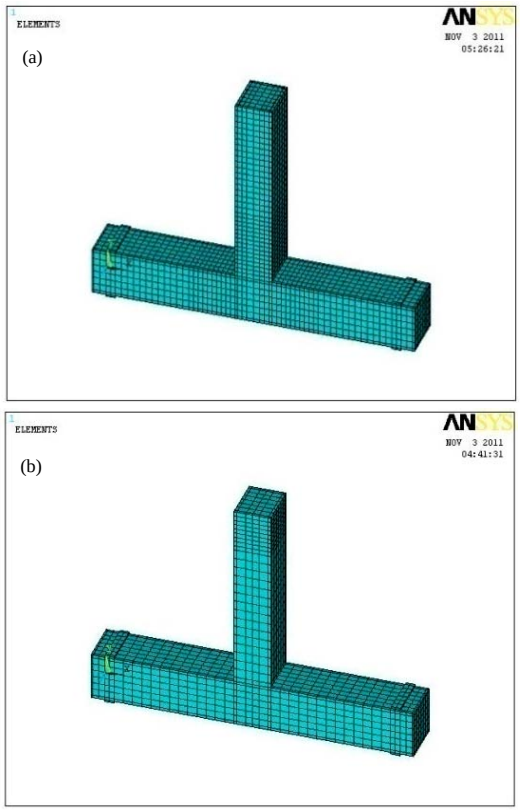


Fig. 15: Models built in ANSYS

365.3 kN.m which shows 7.3% increase compare to J2U connection. As shown in Fig. 16 until the 7 mm displacement the load-displacement curve is the same for both connections. Form 7 mm displacement to 40 mm displacement the difference between moment-displacement curves increases relatively and from 50-140 mm of displacement the difference between the curves of each group increases. In such way that in the first group the maximum moment of J1D specimen is 8.7 more than the maximum moment of specimen J1U. Also in second group the maximum moment supported by J2D model is 7.5 more than J2U. The resulted of FEM analysis of the specimen is shown. Based on the results the displacement in which the first yielding of longitudinal bars is observed is 16.1 mm for J1D specimen from first group which shows 15% reduction in compare to J1U specimen. In the second group for J2D specimen the first

Table 7: Ultimate loading and displacement and ductility coeficient of FEM specimen

| Specimen | $\Delta_y$ (mm) | $M_y$ (kN.m) | $\Delta_u$ (mm) | $M_u$ (kN.m) | $\mu = \Delta_u/\Delta_y$ |
|---|---|---|---|---|---|
| J1D | 16.10 | 57.15 | 140 | 135.6 | 8.69 |
| J1U | 19.05 | 65.60 | 140 | 123.9 | 7.35 |
| J2D | 17.30 | 138.70 | 140 | 365.3 | 8.09 |
| J2U | 21.23 | 142.20 | 140 | 338.6 | 6.59 |

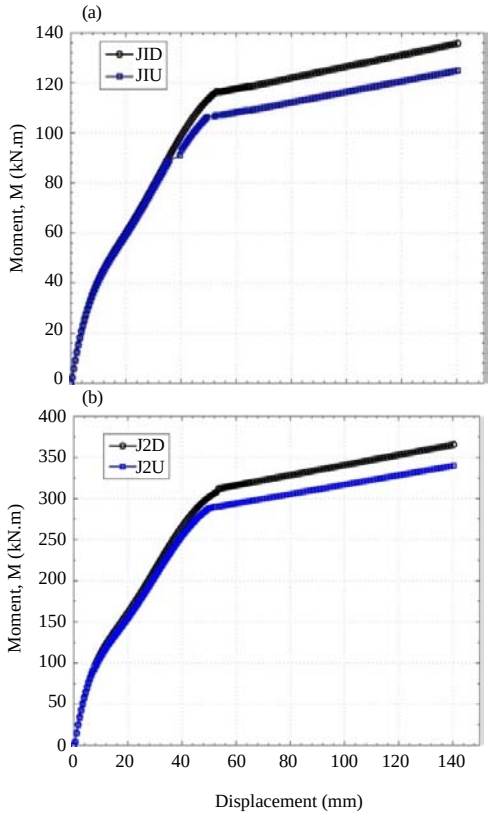


Fig. 16: Force-displacement of two connection groups: a) First group and b) Second group

rebar yielding happened at 17.3 mm displacement which is 19% less than J2U specimen. Based on analysi's result, the first yielding of beam's longitudinal rebar is the least for J1D and the most for J2U among other specimen. Based on Fig. 17 and Table 7 in two groups, the first connection of each group (J1D, J2D) which are enhanced by ductile FRP stirrups have higher ductility coefficient compared to connections without ductile FRP stirrups (J1U, J2U). J1D connection with ductility coefficient is 8.69 which shows a 11.5% increase compared to J1U

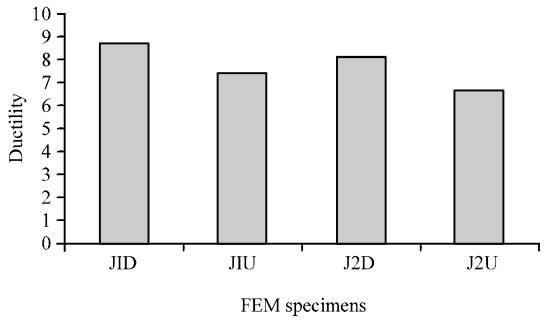


Fig. 17: Changes in ductility of two groups of connections

specimen. Furthermore in the second group J2D has a ductility coefficient of 8.09% which is 22% more than J2U specimen.

## CONCLUSION

Based on the experiments carried on the specimens it was observed that during loading stages no strength reduction happened and almost both connections passed the loading stages with no drop in strength. The first longitudinal rebar yielding in the reference specimen happened at 9.89 mm displacement. The ductility, based on displacement ratio to ultimate displacement ($\Delta_u/\Delta_y$) is 8.6 for reference specimens.

According to results from testing experimental specimen, the maximum observed strain at the end of loading, belonged to stirrups at panel zone equal to 0.24%. The maximum connection rotation for reference specimen is 0.58 rad. Besides the maximum energy absorption for the reference specimen at 7% drift is 3610 kN.mm.

According to FEM analysis to the both groups, using FRP stirrups while considering ductility regulations lead to increase in load bearing capacity, comparing to the situation where spacing between stirrups is more. In such way that in the first group specimen J1D has the maximum moment of 135/6 kN.m which is 8.6% more than J1U specimen. In the second group the J2D connection has the maximum moment of 365.3 kN.m which shows 7.3% increase compare to J2U connection.

Based on FEM analysis carried on models, it was shown that using FRP stirrups with small distances leads in load bearing capacity of FEM specimen.

## REFERENCES

ACI Committee 318, 2002. Building code requirements for structural concrete (ACI 318-02) and commentary (318R-02). ACI, Farmington Hills, MI.

ACI Committee 440.2R-02, 2002. Guide for the design and construction of externally bonded FRP systems for strengthening concrete structures. http://www.concrete.org/bookstorenet/ProductDetail.aspx?SACode=440202.

Canadian Standards Association, 2002. Design and construction of building components with fibre-reinforced polymers. Canadian Standards Association, Mississauga, Canada.

Ceroni, F., 2010. Experimental performances of RC beams strengthened with FRP materials. Constr. Build. Mater., 24: 1547-1559.

Fukuyama, H., Y. Masuda, Y. Sonobe and M. Tanigaki, 1995. Structural Performances of Concrete Frame Reinforced with FRP Reinforcement. In: Rilem Proceedings, Taerwe, E. and F.N. Spon (Eds.) Chapman & Hall, London, UK., pp: 275-286.

Ghobarah, A. and A. Said, 2002. Shear strengthening of beam-column joints. Eng. Struct., 24: 881-888.

Mahini, S.S. and H.R. Ronagh, 2010. Strength and ductility of FRP web-bonded RC beams for the assessment of retrofitted beam-column joints. Composite Struct., 92: 1325-1332.

Mukherjee, A. and M. Joshi, 2005. FRPC reinforced concrete beam-column joints under cyclic excitation. Compos. Struct., 70: 185-199.

Nanni, A., 2001. North America design guidelines for concrete reinforcement and strengthening using FRP: Principles, applications and unresolved issues. Proceedings of the FRP Composites in Civil Engineering Conference, December 12-15, 2001, Hong Kong, pp: 61-72.

Sharbatdar, M. and Kazem, 2003. Concrete columns and beams reinforced with FRP Bars and grids under monotonic and reversed cyclic loading. Ph.D. Thesis, University of Ottawa.

Sharbatdar, M.K., M. Saatcioglu and B. Benmokrane, 2011. Experimental investigation behaviour of concrete connections reinforced with CFRP bars and grids. Compos. Struct., 93: 2439-2449.

Si-Larbi, A., A. Agbossou, E. Ferrier and L. Michel, 2012. Strengthening RC beams with composite fiber cement plate reinforced by prestressed FRP rods: Experimental and numerical analysis. Compos. Struct., 94: 830-838.

Theodorakopoulos, D.D. and R.N. Swamy, 2008. A design model for punching shear of FRP-reinforced slab-column connections. Cem. Concr. Compos., 30: 544-555.